VOLUME 74, NUMBER 4 JOC Featured Article February 20, 2009

Transfer of Noncovalent Chiral Information along an Optically Inactive Helical Peptide Chain: Allosteric Control of Asymmetry of the C-Terminal Site by External Molecule that Binds to the N-Terminal Site

Naoki Ousaka[†,§] and Yoshihito Inai*[,‡]

Department of Environmental Technology and Urban Planning and Department of Frontier Materials, Shikumi College, Graduate School of Engineering, Nagoya Institute of Technology, Gokiso-cho, Showa-ku, Nagoya 466-8555, Japan

inai.yoshihito@nitech.ac.jp

Received August 1, 2008

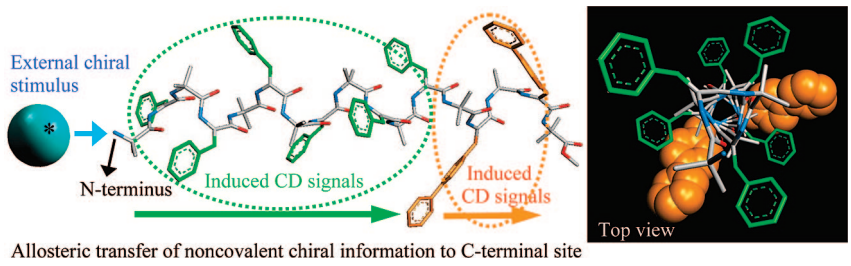

Allosteric transfer of noncovalent chiral information to C-terminal site

This study aims at demonstrating end-to-end transfer of noncovalent chiral information along a peptide chain. The domino-type induction of helical sense is proven by using achiral peptides **1**-*m* of bis-chromophoric sequence with different chain lengths: H-(Aib-Δ^ZPhe)$_m$-(Aib-Δ^ZBip)$_2$-Aib-OCH$_3$ [*m* = 2, 4, and 6; Aib = α-aminoisobutyric acid; Δ^ZPhe = (*Z*)-α,*β*-didehydrophenylalanine; Δ^ZBip = (*Z*)-*β*-(4,4′-biphenyl)-α,*β*-didehydroalanine]. They all showed the tendency to adopt a 3_{10}-helix. Whereas peptide **1**-*m* originally shows no circular dichroism (CD) signals, marked CD signals were induced at around 270−320 nm based on both the *β*-aryl didehydroresidues by chiral Boc-proline (Boc = *tert*-butoxycarbonyl). The observed CD spectra were interpreted on the basis of the exciton chirality method and theoretical CD simulation of several helical conformations that were energy-minimized. The experimental and theoretical CD analysis reveals that Boc-L-proline induces the preference for a right-handed helicity in the whole chain of **1**-*m*. Such noncovalent chiral induction was not observed in the corresponding N-terminally protected **1**-*m*. Obviously, helicity induction in **1**-*m* originates from the binding of Boc-proline to the N-terminal site. In the 17-mer (**1**-*6*), the information of helix sense reaches the 16th residue from the N-terminus. We have monitored precise transfer of noncovalent chiral stimulus along a helical peptide chain. The present study also proposes a primitive allosteric model of a single protein-mimicking backbone. Here chiral molecule binding the N-terminal site of **1**-*6* controls the chiroptical signals and helical sense of the C-terminal site about 30 Å away.

Introduction

Tertiary structures of biopolymers are expressed as asymmetric information originating from their backbone torsion. A helical structure cooperatively integrates chiral information of each constituent into a linear chain.[1] The transfer of chiral information

[†] Department of Environmental Technology and Urban Planning.

[‡] Department of Frontier Materials.

[§] Present address: JST ERATO-SORST Kuroda Chiromorphology Team.

10.1021/jo801686m CCC: $40.75 © 2009 American Chemical Society
Published on Web 11/19/2008

along a helical chain plays a key role for nucleation, propagation, and termination of a one-handed helicity ubiquitous in asymmetric living organisms.[2−4]

Control of helical sense has been extensively investigated using artificial helical models based on achiral monomer units.[1,5−8] Here the helical sense of such an optically inactive segment is induced by covalent or noncovalent chiral stimuli.[1,5−8] These leading studies provide significant guidance as to how chiral information transfers along a molecular chain to generate a one-handed helix. Such an optically inactive helix usually involves chromophoric groups in the main chain or side chain. Electronic circular dichroism (CD) spectroscopy that focuses on these chromophores can clarify a helical sense induced in the backbone itself. Furthermore, elegant studies on artificial helical backbones have been reported in which helix propagation or reversal is visually detected.[9] However, chiral stimulus is hardly traceable on biopolymer frameworks, especially on *protein backbones*, because their chemically chiral sequences prevent us from monitoring transfer of site-specific chiral information.

We have proposed noncovalent chiral induction in optically inactive helical peptides as a protein-mimicking backbone.[10−12] Such sequences are composed primarily of unusual achiral α-amino acids, whereby we can extract information of a helix sense triggered by chiral stimulus. The N-terminal-free segment binds chiral molecules such as N-terminally blocked amino acid and peptide acid. A terminal twist originating in the formation of the chiral complex gives rise to energy imbalance between the two enantiomeric helices.[12] Dynamic chiral information at the N-terminal site induces the preference for a helical sense. We have figuratively termed this phenomenon the noncovalent chiral domino effect (NCDE).[10b,12] Helix-sense induction of an achiral linear segment also occurs through covalent incorporation

(1) For elegant articles of helical polymers, see: (a) Hill, D. J.; Mio, M. J.; Prince, R. B.; Hughes, T. S.; Moore, J. S. *Chem. Rev.* **2001**, *101*, 3893–4011. (b) Green, M. M.; Park, J.-W.; Sato, T.; Teramoto, A.; Lifson, S.; Selinger, R. L. B.; Selinger, J. V. *Angew. Chem., Int. Ed.* **1999**, *38*, 3138–3154. (c) Nakano, T.; Okamoto, Y. *Chem. Rev.* **2001**, *101*, 4013–4038. (d) Yashima, E.; Maeda, K.; Nishimura, T. *Chem. Eur. J.* **2004**, *10*, 42–51. (e) Brunsveld, L.; Folmer, B. J. B.; Meijer, E. W.; Sijbesma, R. P. *Chem. Rev.* **2001**, *101*, 4071–4097. (f) Cornelissen, J. J. L. M.; Rowan, A. E.; Nolte, R. J. M.; Sommerdijk, N. A. J. M. *Chem. Rev.* **2001**, *101*, 4039–4070. (g) Dolain, C.; Léger, J.-M.; Delsuc, N.; Gornitzka, H.; Huc, I. *Proc. Natl. Acad. Sci. U.S.A.* **2005**, *102*, 16146–16151.

(2) (a) Aurora, R.; Srinivasan, R.; Rose, G. D. *Science* **1994**, *264*, 1126–1130. (b) Schellman, C. In *Protein Folding*; Jaenicke, R., Ed.; North-Holland Biomedical Press, Elsevier: Amsterdam, 1980; pp 53−61. (c) Sagermann, M.; Mårtensson, L.-G.; Baase, W. A.; Matthews, B. W. *Protein Sci.* **2002**, *11*, 516–521. (d) Jiménez, M. A.; Muñoz, V.; Rico, M.; Serrano, L. *J. Mol. Biol.* **1994**, *242*, 487–496. (e) Harper, E. T.; Rose, G. D. *Biochemistry* **1993**, *32*, 7605–7609. (f) Kim, P. S.; Baldwin, R. L. *Nature* **1984**, *307*, 329–334. (g) Storrs, R. W.; Truckses, D.; Wemmer, D. E. *Biopolymers* **1992**, *32*, 1695–1702. (h) Lawrence, J. R.; Johnson, W. C. *Biophys. Chem.* **2002**, *101*−*102*, 375–385. (i) Monticelli, L.; Tieleman, D. P.; Colombo, G. *J. Phys. Chem. B* **2005**, *109*, 20064–20067. For C-terminal hydrogen-bonding patterns of helical model peptides, see also: (j) Datta, S.; Uma, M. V.; Shamala, N.; Balaram, P. *Biopolymers* **1999**, *50*, 13–22. (k) Benedetti, E.; Di Blasio, B.; Pavone, V.; Pedone, C.; Santini, A.; Bavoso, A.; Toniolo, C.; Crisma, M.; Sartore, L. *J. Chem. Soc., Perkin Trans. 2* **1990**, 1829–1837.

(3) For insightful simulation of heterochiral/homochiral helices, see: (a) Nanda, V.; DeGrado, W. F. *J. Am. Chem. Soc.* **2004**, *126*, 14459–14467. (b) Nanda, V.; DeGrado, W. F. *J. Am. Chem. Soc.* **2006**, *128*, 809–816.

(4) Kuroda, R. *Enantiomer* **2000**, *5*, 439–450.

(5) For leading examples of covalent chiral effects on helix sense, see: (a) Green, M. M.; Reidy, M. P.; Johnson, R. D.; Darling, G.; O'Leary, D. J.; Willson, G. *J. Am. Chem. Soc.* **1989**, *111*, 6452–6454. (b) Tian, G.; Lu, Y.; Novak, B. M. *J. Am. Chem. Soc.* **2004**, *126*, 4082–4083. (c) Tang, H.-Z.; Lu, Y.; Tian, G.; Capracotta, M. D.; Novak, B. M. *J. Am. Chem. Soc.* **2004**, *126*, 3722–3723. (d) Dolain, C.; Jiang, H.; Léger, J.-M.; Guionneau, P.; Huc, I. *J. Am. Chem. Soc.* **2005**, *127*, 12943–12951. (e) Okamoto, Y.; Matsuda, M.; Nakano, T.; Yashima, E. *Polym. J.* **1993**, *25*, 391–396. (f) Maeda, K.; Okamoto, Y. *Polym. J.* **1998**, *30*, 100−105. (g) Nath, G. Y.; Samal, S.; Park, S.-Y.; Murthy, C. N.; Lee, J.-S. *Macromolecules* **2006**, *39*, 5965–5966. (h) Tabei, J.; Shiotsuki, M.; Sato, T.; Sanda, F.; Masuda, T. *Chem. Eur. J.* **2005**, *11*, 3591−3598. (i) Kamer, P. C. J.; Cleij, M. C.; Nolte, R. J. M.; Harada, T.; Hezemans, A. M. F.; Drenth, W. *J. Am. Chem. Soc.* **1988**, *110*, 1581–1587.

(6) (a) Prince, R. B.; Barnes, S. A.; Moore, J. S. *J. Am. Chem. Soc.* **2000**, *122*, 2758–2762. (b) Yashima, E.; Matsushima, T.; Okamoto, Y. *J. Am. Chem. Soc.* **1997**, *119*, 6345–6359. (c) Yashima, E.; Maeda, K.; Okamoto, Y. *Nature* **1999**, *399*, 449–451. (d) Maeda, K.; Ishikawa, M.; Yashima, E. *J. Am. Chem. Soc.* **2004**, *126*, 15161–15166. (e) Schlitzer, D. S.; Novak, B. M. *J. Am. Chem. Soc.* **1998**, *120*, 2196–2197. (f) Maurizot, V.; Dolain, C.; Huc, I. *Eur. J. Org. Chem.* **2005**, *2005*, 1293–1301. (g) Majidi, M. R.; Kane-Maguire, L. A. P.; Wallace, G. G. *Polymer* **1994**, *35*, 3113–3115. (h) Green, M. M.; Khatri, C.; Peterson, N. C. *J. Am. Chem. Soc.* **1993**, *115*, 4941–4942. (i) Nakashima, H.; Koe, J. R.; Torimitsu, K.; Fujiki, M. *J. Am. Chem. Soc.* **2001**, *123*, 4847–4848.

(7) For transfer of chiral information in supramolecular assemblies, see: (a) Smulders, M. M. J.; Schenning, A. P. H. J.; Meijer, E. W. *J. Am. Chem. Soc.* **2008**, *130*, 606–611. (b) van Gestel, J.; Palmans, A. R. A.; Titulaer, B.; Vekemans, J. A. J. M.; Meijer, E. W. *J. Am. Chem. Soc.* **2005**, *127*, 5490–5494. (c) Lauceri, R.; Raudino, A.; Scolaro, L. M.; Micali, N.; Purrello, R. *J. Am. Chem. Soc.* **2002**, *124*, 894–895. (d) Mammana, A.; D'Urso, A.; Lauceri, R.; Purrello, R. *J. Am. Chem. Soc.* **2007**, *129*, 8062–8063. (e) Prins, L. J.; Timmerman, P.; Reinhoudt, D. N. *J. Am. Chem. Soc.* **2001**, *123*, 10153–10163.

(8) For biorelated helical backbones, see: (a) Kozlov, I. A.; Orgel, L. E.; Nielsen, P. E. *Angew. Chem., Int. Ed.* **2000**, *39*, 4292–4295. (b) Mazaleyrat, J.-P.; Wright, K.; Gaucher, A.; Toulemonde, N.; Wakselman, M.; Oancea, S.; Peggion, C.; Formaggio, F.; Setnička, V.; Keiderling, T. A.; Toniolo, C. *J. Am. Chem. Soc.* **2004**, *126*, 12874–12879. (c) Benedetti, E.; Saviano, M.; Iacovino, R.; Pedone, C.; Santini, A.; Crisma, M.; Formaggio, F.; Toniolo, C.; Broxterman, Q. B.; Kamphuis, J. *Biopolymers* **1998**, *46*, 433–443. (d) Benedetti, E.; Saviano, M.; Iacovino, R.; Crisma, M.; Formaggio, F.; Toniolo, C. *Z. Kristallogr.* **1999**, *214*, 160–166. (e) Crisma, M.; Valle, G.; Formaggio, F.; Toniolo, C. *Z. Kristallogr.* **1998**, *213*, 599–604. (f) Pengo, B.; Formaggio, F.; Crisma, M.; Toniolo, C.; Bonora, G. M.; Broxterman, Q. B.; Kamphuis, J.; Saviano, M.; Iacovino, R.; Rossi, F.; Benedetti, E. *J. Chem. Soc., Perkin Trans. 2* **1998**, 1651–1657. (g) Pieroni, O.; Fissi, A.; Pratesi, C.; Temussi, P. A.; Ciardelli, F. *J. Am. Chem. Soc.* **1991**, *113*, 6338–6340. (h) Tuzi, A.; Ciajolo, M. R.; Guarino, G.; Temussi, P. A.; Fissi, A.; Pieroni, O. *Biopolymers* **1993**, *33*, 1111–1121. (i) Pieroni, O.; Fissi, A.; Pratesi, C.; Temussi, P. A.; Ciardelli, F. *Biopolymers* **1993**, *33*, 1–10. (j) Ramagopal, U. A.; Ramakumar, S.; Joshi, R. M.; Chauhan, V. S. *J. Pept. Res.* **1998**, *52*, 208–215.

(9) (a) Sone, E. D.; Zubarev, E. R.; Stupp, S. I. *Angew. Chem., Int. Ed.* **2002**, *41*, 1705–1709. (b) Sakurai, S.; Ohsawa, S.; Nagai, K.; Okoshi, K.; Kumaki, J.; Yashima, E. *Angew. Chem., Int. Ed.* **2007**, *46*, 7605–7608. (c) Sakurai, S.; Okoshi, K.; Kumaki, J.; Yashima, E. *J. Am. Chem. Soc.* **2006**, *128*, 5650–5651. (d) Maeda, T.; Furusho, Y.; Sakurai, S.; Kumaki, J.; Okoshi, K.; Yashima, E. *J. Am. Chem. Soc.* **2008**, *130*, 7938–7945. (e) Shinohara, K.; Yasuda, S.; Kato, G.; Fujita, M.; Shigekawa, H. *J. Am. Chem. Soc.* **2001**, *123*, 3619–3620.

(10) (a) Inai, Y.; Tagawa, K.; Takasu, A.; Hirabayashi, T.; Oshikawa, T.; Yamashita, M. *J. Am. Chem. Soc.* **2000**, *122*, 11731–11732. (b) Inai, Y.; Ousaka, N.; Okabe, T. *J. Am. Chem. Soc.* **2003**, *125*, 8151–8162. (c) Ousaka, N.; Inai, Y.; Okabe, T. *Biopolymers* **2006**, *83*, 337–351. (d) Inai, Y.; Hirano, T. *ITE Lett. Batteries, New Technol. Med.* **2003**, *4*, 485–488. (e) Inai, Y.; Ousaka, N.; Ookouchi, Y. *Biopolymers* **2006**, *82*, 471–481.

(11) For the control of helix sense of sequence containing chiral residue, see: (a) Inai, Y.; Ishida, Y.; Tagawa, K.; Takasu, A.; Hirabayashi, T. *J. Am. Chem. Soc.* **2002**, *124*, 2466–2473. (b) Inai, Y.; Komori, H.; Takasu, A.; Hirabayashi, T. *Biomacromolecules* **2003**, *4*, 122–128. (c) Inai, Y.; Komori, H. *Biomacromolecules* **2004**, *5*, 1231–1240. (d) Komori, H.; Inai, Y. *J. Org. Chem.* **2007**, *72*, 4012–4022.

(12) Inai, Y.; Komori, H.; Ousaka, N. *Chem. Rec.* **2007**, *7*, 191–202.

(13) (a) Ousaka, N.; Inai, Y. *J. Am. Chem. Soc.* **2006**, *128*, 14736–14737. (b) Inai, Y.; Ashitaka, S.; Hirabayashi, T. *Polym. J.* **1999**, *31*, 246–253.

(14) Aib^{14a-h} or $\Delta^{Z}Phe^{14i-p}$ residues incorporated into a peptide sequence tend to promote the 3_{10}-/α-helical propensity: (a) Karle, I. L.; Gopi, H. N.; Balaram, P. *Proc. Natl. Acad. Sci. U.S.A.* **2003**, *100*, 13946–13951. (b) Venkatraman, J.; Shankaramma, S. C.; Balaram, P. *Chem. Rev.* **2001**, *101*, 3131–3152. (c) Karle, I. L.; Flippen-Anderson, J. L.; Uma, K.; Balaram, H.; Balaram, P. *Proc. Natl. Acad. Sci. U.S.A.* **1989**, *86*, 765–769. (d) Benedetti, E.; Bavoso, A.; Di Blasio, B.; Pavone, V.; Pedone, C.; Crisma, M.; Bonora, G. M.; Toniolo, C. *J. Am. Chem. Soc.* **1982**, *104*, 2437–2444. (e) Yanagisawa, K.; Morita, T.; Kimura, S. *J. Am. Chem. Soc.* **2004**, *126*, 12780–12781. (f) Okuyama, K.; Saga, Y.; Nakayama, M.; Narita, M. *Biopolymers* **1991**, *31*, 975–985. (g) Toniolo, C.; Benedetti, E. *Trends Biochem. Sci.* **1991**, *16*, 350–353. (h) Toniolo, C.; Bonora, G. M.; Bavoso, A.; Benedetti, E.; Di Blasio, B.; Pavone, V.; Pedone, C. *Biopolymers* **1983**, *22*, 205–215. (i) Rajashankar, K. R.; Ramakumar, S.; Chauhan, V. S. *J. Am. Chem. Soc.* **1992**, *114*, 9225–9226. (j) Jain, R. M.; Rajashankar, K. R.; Ramakumar, S.; Chauhan, V. S. *J. Am. Chem. Soc.* **1997**, *119*, 3205–3211. (k) Ramagopal, U. A.; Ramakumar, S.; Sahal, D.; Chauhan, V. S. *Proc. Natl. Acad. Sci. U.S.A.* **2001**, *98*, 870–874. (l) Ciajolo, M. R.; Tuzi, A.; Pratesi, C. R.; Fissi, A.; Pieroni, O. *Biopolymers* **1990**, *30*, 911–920. (m) Ciajolo, M. R.; Tuzi, A.; Pratesi, C. R.; Fissi, A.; Pieroni, O. *Biopolymers* **1992**, *32*, 717–724. (n) Mitra, S. N.; Dey, S.; Karthikeyan, S.; Singh, T. P. *Biopolymers* **1997**, *41*, 97–105. (o) Chauhan, V. S.; Uma, K.; Kaur, P.; Balaram, P. *Biopolymers* **1989**, *28*, 763–771. (p) Gupta, A.; Bharadwaj, A.; Chauhan, V. S. *J. Chem. Soc., Perkin Trans. 2* **1990**, 1911–1916.

SCHEME 1. Achiral Peptides 1-*m* [H-(Aib-Δ^ZPhe)$_m$-(Aib-Δ^ZBip)$_2$-Aib-OMe, m = 2, 4, and 6], 2 [H-(Aib-Δ^ZBip)$_4$-Aib-OMe], and 3 [H-(Aib-Δ^ZPhe)$_4$-Aib-OMe] for the NCDE Study[a]

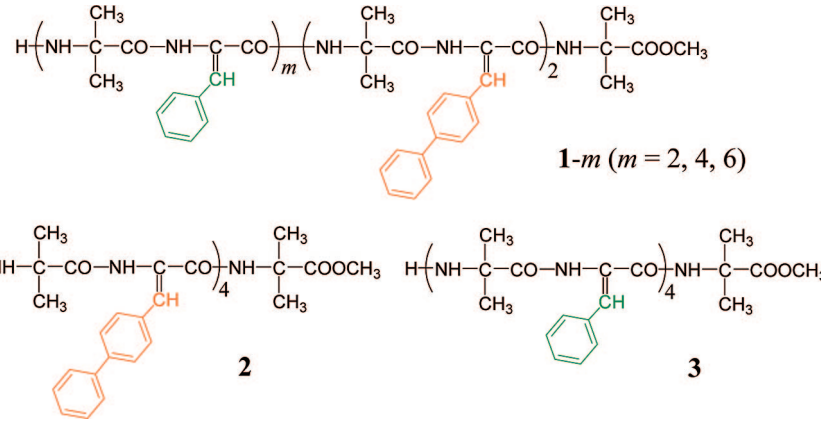

[a] Induction of helical sense in peptide **3** through noncovalent chiral interaction was reported in ref 10a.

of chiral moieties into the terminal site[5d−g,8b,f−h,j,13] and can be termed the covalent chiral domino effect (CCDE).[10b,12]

Our NCDE experiments have not offered the precise route, because the electronic CD spectroscopy focuses on the same chromophores incorporated in the sequence. Here, achiral alternating sequences of (*Z*)-α,*β*-didehydrophenylalanine (Δ^ZPhe) and α-aminoisobutyric acid (Aib) have been used for design of the optically inactive helical segment.[10−16] The Δ^ZPhe chromophore is characterized by a strong absorption band at around 280 nm, in which the transition dipole moment (TDM) places roughly at the phenyl−carbonyl line.[17] According to the exciton chirality method,[18] split-type CD patterns at around 280 nm are predicted for a -Δ^ZPhe-X-Δ^ZPhe- segment in a helical conformation. This was true in chiral stimulus-induced CD spectra of nonapeptides based on (Δ^ZPhe-X)$_n$.[10,11,13,17d] We have interpreted the CD spectra as helical sense induced in the whole molecule. However, such split CD patterns do not always mean a preference for a one-handed helix in the *entire* chain. They can be derived merely from a *local* Δ^ZPhe−Δ^ZPhe twist. In this regard, we have not directly proven the NCDE that chain-terminal chiral information spreads over the entire chain. Helix propagation and termination are detected in elegant artificial molecules.[8f,9,19] However, it is still unclear on a single protein-mimicking chain composed of α-amino acids that dynamic chiral information transfers from one chain terminus to the opposite end.

The present study aims at demonstrating that chiral stimulus received at the N-terminus of achiral peptide is truly transferred to the C-terminal region. The position-specific incorporation of some chromophores offers conformational information about a local chain.[20] Hence we have designed alternating sequences **1**-*m* of Aib with two types of *β*-aryl didehydroalanine (ΔAA) residues, illustrated in Scheme 1. Peptides **1**-*m* are characterized by the Δ^ZPhe-based region with different chain lengths, with their C-terminal connected to a pair of (*Z*)-4,4′-biphenyl-α,*β*-didehydroalanine (Δ^ZBip) residues. The Δ^ZBip residue extends the *π*-conjugation system of Δ^ZPhe moiety to a biphenyl moiety, thus shifting the electronic transition to a longer wavelength. In addition, the TDM direction of the Δ^ZBip should roughly resemble that in the Δ^ZPhe case[17a,c] due to similar symmetry in rotation about the $C^\beta-C^\gamma$ bond. A spatially twisted Δ^ZBip−Δ^ZBip pair will function as an efficient CD probe at wavelengths different from those of the electronic transition of Δ^ZPhe residues. As a result, if the helicity induction occurs at the whole molecular level, CD signals will be detected simultaneously on both the Δ^ZPhe and Δ^ZBip residues. Notably, CD signals for the latter chromophore provide direct evidence for transfer of N-terminal chiral information to the C-terminal region.

We also propose a primitive model for allosteric proteins in which molecular binding at one site leads to control of structure or activity of another remote region.[21] Such remote control not only is found in biological functions but also is elegantly demonstrated in synthetic receptors or catalysts.[22] In our present model, an external chiral molecule should stimulate the N-terminal site of **1**-*m* to induce chiroptical signals and helical sense of the C-terminal region. If this allosteric control successfully occurs on **1**-*6* in a 3_{10}-helix,[23] the Aib(1)−Δ^ZBip(16) distance would be beyond 30 Å. This controllable distance is comparable to the most efficient case in a synthetic unimolecule.[19a]

(15) (a) Inai, Y.; Oshikawa, T.; Yamashita, M.; Tagawa, K.; Hirabayashi, T. *Biopolymers* **2003**, *70*, 310–322. (b) Inai, Y.; Oshikawa, T.; Yamashita, M.; Hirabayashi, T.; Ashitaka, S. *J. Chem. Soc., Perkin. Trans. 2* **2001**, 892–897.

(16) Nandel, F. S.; Khare, B. *Biopolymers* **2005**, *77*, 63–73.

(17) For CD and absorption studies for Δ^ZPhe-containing peptides, see: (a) Pieroni, O.; Fissi, A.; Jain, R. M.; Chauhan, V. S. *Biopolymers* **1996**, *38*, 97–108. (b) Pieroni, O.; Montagnoli, G.; Fissi, A.; Merlino, S.; Ciardelli, F. *J. Am. Chem. Soc.* **1975**, *97*, 6820–6826. (c) Inai, Y.; Ito, T.; Hirabayashi, T.; Yokota, K. *Biopolymers* **1993**, *33*, 1173–1184. For CD spectra simulated for helical sequence based on -(X-Δ^ZPhe)$_n$-, see: (d) Komori, H.; Inai, Y. *J. Phys. Chem. A* **2006**, *110*, 9099–9107.

(18) For the exciton chirality method, see: (a) Harada, N.; Chen, S. L.; Nakanishi, K. *J. Am. Chem. Soc.* **1975**, *97*, 5345–5352. (b) Harada, N.; Nakanishi, K. *Circular Dichroic Spectroscopy. Exciton Coupling in Organic Stereochemistry*; University Science Books: Mill Valley, CA, 1983.

(19) Elegant models have been proposed for the remote control of conformational information along a molecular frame: (a) Clayden, J.; Lund, A.; Vallverdú, L.; Helliwell, M. *Nature* **2004**, *431*, 966–971. (b) Mizutani, T.; Sakai, N.; Yagi, S.; Takagishi, T.; Kitagawa, S.; Ogoshi, H. *J. Am. Chem. Soc.* **2000**, *122*, 748–749.

(20) (a) Johnson, N. P.; Baase, W. A.; von Hippel, P. H. *Proc. Natl. Acad. Sci. U.S.A.* **2004**, *101*, 3426–3431. (b) Johnson, N. P.; Baase, W. A.; von Hippel, P. H. *Proc. Natl. Acad. Sci. U.S.A.* **2005**, *102*, 7169–7173. (c) Inai, Y.; Sisido, M.; Imanishi, Y. *J. Phys. Chem.* **1990**, *94*, 6237–6243. (d) Inai, Y.; Sisido, M.; Imanishi, Y. *J. Phys. Chem.* **1990**, *94*, 8365–8370.

(21) For allosteric proteins, see: Monod, J.; Changeux, J. P.; Jacob, F. *J. Mol. Biol.* **1963**, *6*, 306–329.

(22) (a) Shinkai, S.; Ikeda, M.; Sugasaki, A.; Takeuchi, M. *Acc. Chem. Res.* **2001**, *34*, 494–503. (b) Takeuchi, M.; Ikeda, M.; Sugasaki, A.; Shinkai, S. *Acc. Chem. Res.* **2001**, *34*, 865–873. (c) Kovbasyuk, L.; Krämer, R. *Chem. Rev.* **2004**, *104*, 3161–3187.

(23) The simulated 3_{10}-helical structure is shown later (Figure 3). For structural features of the 3_{10}-helix, see ref 14g. See also: Barlow, D. J.; Thornton, J. M. *J. Mol. Biol.* **1988**, *201*, 601–619.

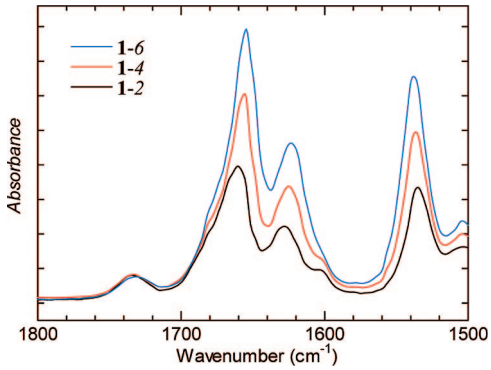

FIGURE 1. FT-IR absorption spectra of **1**-*6* in chloroform/methanol (95/5, v/v %) and **1**-*4* and **1**-*2* in chloroform at ambient temperature: [peptide] = 3 mM.

A quick overview of the work is as follows. In peptides **1**-*m*, chiral Boc-proline induced CD signals at both absorption bands of the Δ^ZPhe and Δ^ZBip residues.[24] These CD results have been compared with the helicity induction of nonapeptide **2** or **3**[10a] based on either the Δ^ZBip or Δ^ZPhe chromophores, respectively. In addition, the spectral patterns observed have been interpreted on the basis of simulations of electronic transition states and theoretical CD spectra. In conclusion, the NCDE can control the helical sense of the entire chain substantially. In the 17-mer ($m = 6$), chiral information reaches the 16th residue, thus demonstrating long-range allosteric control in a protein-mimicking helical backbone.

Results and Discussion

Helical Conformations of Peptides 1-*m*. It has been widely revealed that incorporation of Aib or Δ^ZPhe residues promotes helical propensity.[14] Sequences based on -Aib-Δ^ZPhe- or -Δ^ZPhe-Aib- are shown to adopt a 3_{10}-helix in solution and crystalline form, and on theoretical basis.[10−16] Particularly, a 3_{10}-helix is found in peptide **3** or its N-Boc-protected form as analogs of **1**-*m*.[10a,12,15a] In addition, conformational space of other ΔAA residues resembles that of Δ^ZPhe.[25] For instance, oligopeptides containing two or more (*Z*)-α,*β*-didehydronaphthylalanine residues tend to take a 3_{10}-helical conformation.[25b] Furthermore, a biphenyl side chain can be placed on a helical peptide backbone.[26]

The preliminary information suggests the propensity for a helical structure in **1**-*m*. For the experimental evidence, FT-IR absorption spectra of **1**-*m* in chloroform are displayed in Figure 1, focusing on the amide I and II regions.

Two prominent absorption bands were commonly seen in the amide I region. These peak positions are summarized in Table 1.[27] Similar patterns are observed for analogous helical sequences repeating -(X-Δ^ZPhe)-[10a−d,11a−c,28]. In particular, such an amide pattern is seen in analogous nonapeptide [Boc-(Aib-Δ^ZPhe)$_4$-Aib-OMe], which adopts a typical 3_{10}-helix in the crystal state.[15a] These peaks have been assigned to carbonyl stretching modes in a helical conformation,[28] being observed at higher wavenumbers for saturated residues and at lower wavenumbers for Δ^ZPhe residues. Peptides **2** and **3** also showed a similar amide I profile.[28] For amide II region, all peptides gave a strong absorption band at 1535−1538 cm^{-1}, of which the position is also observed in Aib-containing oligopeptides.[28b] Therefore peptides **1**-*m* and **2** favor a helical conformation in chloroform.

TABLE 1. Peak Positions[a] Selected in Amide I and II Absorption Bands of Peptides 1-*m*, 2, and 3 in Chloroform[27]

peptide	amide I		amide II
1-*6*	1655	1624	1538
1-*4*	1656	1625	1537
1-*2*	1660	1628	1535
2	1661	1629	1535
3	1660	1629	1535

[a] In cm^{-1}.

Peptides containing Aib or ΔAA residues tend to take a 3_{10}-helix or an α-helix.[14] To identify the helix type, temperature changes in amide NH resonances are shown in Figure 2.[30] When peptide **1**-*m* adopts a 3_{10}-helix, two amide NH groups of the N-terminal sequence lack hydrogen-bonding partners. In the case of an α-helix, three N-terminal amide NHs are free from intramolecular hydrogen bonding. In ^{1}H NMR spectra of **1**-*m* (Figure S2 Supporting Information), NH protons of ΔAA appeared at a considerably lower magnetic field.[29] Thus, the singlets above 8.9 ppm should be assigned to the ΔAA NH protons, of which the number was estimated from relative intensity to be 3 (**1**-*2*), 5 (**1**-*4*), and 7 (**1**-*6*). In each case, one NH proton of ΔAA was not clearly found. This trend is often observed in analogous helical peptides having an N-terminal moiety of H-X-Δ^ZPhe(2)-, where the Δ^ZPhe NH resonance does not appear clearly in $CDCl_3$.[10b,c,11b−d,31] Thus, the lacking NH should be assigned to the Δ^ZPhe(2)'s.

In contrast, the singlets at around 7.9−8.4 ppm should be assigned to the Aib NH groups, of which the numbers were similarly estimated to be 3 (**1**-*2*), 5 (**1**-*4*), and 7 (**1**-*6*). In each case, NOESY cross peaks allow us to identify one remaining Aib NH in a higher magnetic field (Figures S3−S5, Supporting Information). The Aib NH group showed the largest temperature coefficient among the amide groups observed (Figure 2). The identification of a helical conformation from the FT-IR absorp-

(24) Our present study mainly aims at clarifying whether noncovalent chiral information received at the N-terminal site of a chiral peptide is indeed transferred to the C-terminal site. Effects of the N-terminal amino acid or of another Boc-amino acid are not the current issue. These effects on induction of helicity were already reported.[10] Peptide **3** and analogous peptides H-X-(Δ^ZPhe-Aib)$_4$-OMe (X = Aib, *β*-Ala, Gly, or *N*-methylglycine) commonly underwent induction of a right-handed helix through addition of Boc-L-Y-OH (Y = Pro, Leu, Ala, or Val).[10a−d] Thus the choice of the N-terminal amino acid or Boc-amino acid is not an essential factor in the current theme.

(25) (a) Inai, Y.; Oshikawa, T.; Yamashita, M.; Hirabayashi, T.; Hirako, T. *Biopolymers* **2001**, *58*, 9–19. (b) Inai, Y.; Hirabayashi, T. *Biopolymers* **2001**, *59*, 356–369. (c) Inai, Y.; Oshikawa, T.; Yamashita, M.; Hirabayashi, T.; Kurokawa, Y. *Bull. Chem. Soc. Jpn.* **2001**, *74*, 959–966.

(26) (a) Kuragaki, M.; Sisido, M. *J. Phys. Chem.* **1996**, *100*, 16019–16025. (b) Butterfield, S. M.; Patel, P. R.; Waters, M. L. *J. Am. Chem. Soc.* **2002**, *124*, 9751–9755.

(27) Although FT-IR absorption data of peptide **3** were reported in ref 10a, the data have been updated here. FT-IR absorption spectra of **2** and **3** are shown in Figure S1, Supporting Information.

(28) (a) Inai, Y.; Sakakura, Y.; Hirabayashi, T. *Polym. J.* **1998**, *30*, 828–832. (b) Kennedy, D. F.; Crisma, M.; Toniolo, C.; Chapman, D. *Biochemistry* **1991**, *30*, 6541–6548. For IR absorption studies on other peptides possessing Δ^ZPhe residues, see: (c) Gupta, A.; Mehrotra, R.; Tewari, J.; Jain, R. M.; Chauhan, V. S. *Biopolymers* **1999**, *50*, 595–601.

(29) For example, see refs 10, 11, 13, 14o, 14p, and 15.

(30) For intramolecular hydrogen-bonding NH and temperature coefficient, see: (a) Andersen, N. H.; Neidigh, J. W.; Harris, S. M.; Lee, G. M.; Liu, Z.; Tong, H. *J. Am. Chem. Soc.* **1997**, *119*, 8547–8561. (b) Baxter, N. J.; Williamson, M. P. *J. Biomol. NMR* **1997**, *9*, 359–369. (c) Stevens, E. S.; Sugawara, N.; Bonora, G. M.; Toniolo, C. *J. Am. Chem. Soc.* **1980**, *102*, 7048–7050.

(31) This might be partly due to conformational fluctuation of the N-terminal site that does not participate in intramolecular hydrogen bonds. In fact, the Δ^ZPhe(2) NH resonance appears at a lower magnetic field through addition of Boc-amino acid that is hydrogen-bonded to the N-terminal site.[10b,c]

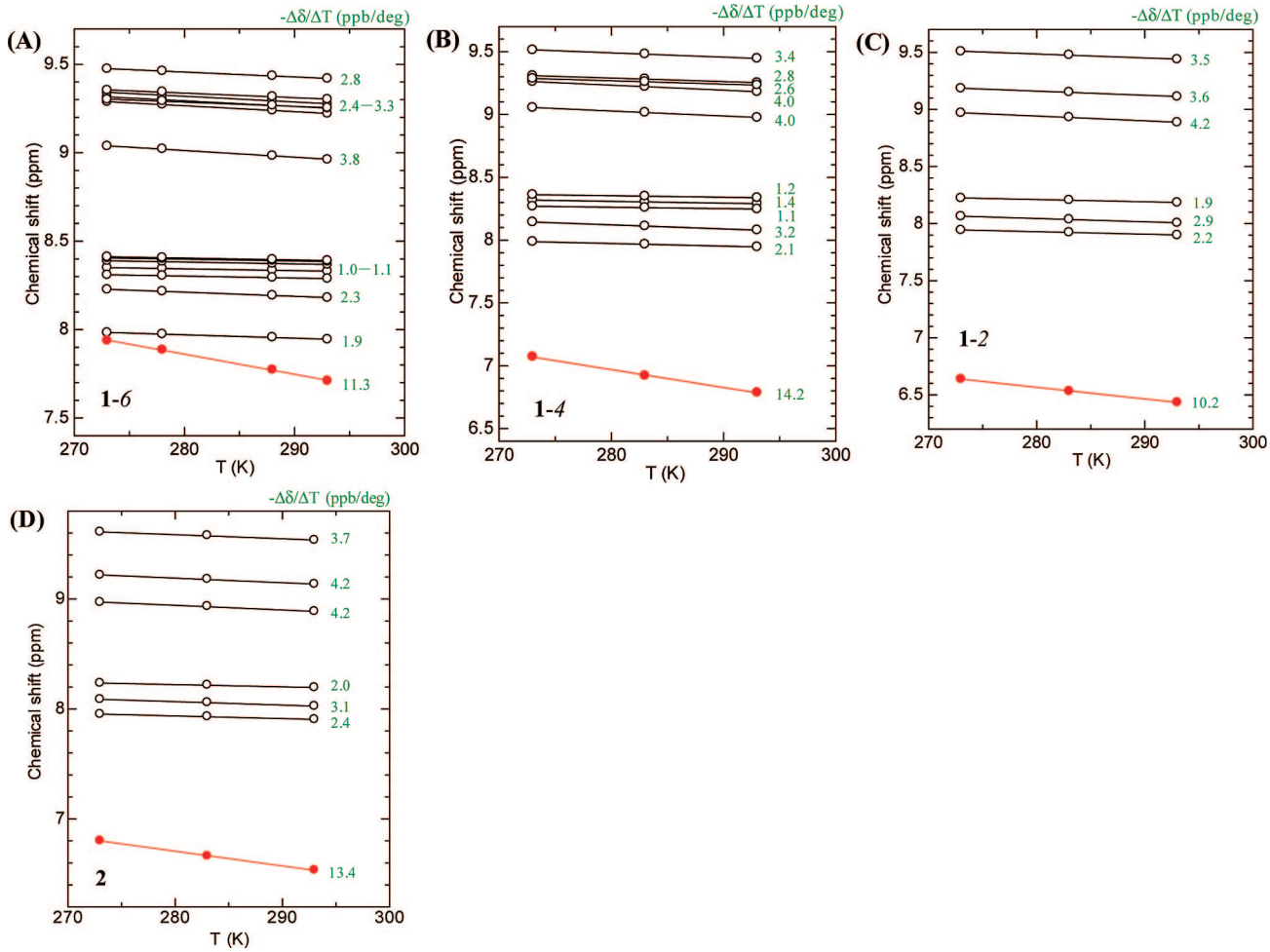

FIGURE 2. Temperature dependence of NH chemical shifts of (A) **1**-*6*, (B) **1**-*4*, (C) **1**-*2*, and (D) **2**: $CDCl_3/(CD_3)_2SO$ (100/3.7, v/v %) for (A); $CDCl_3$ for (B)−(D). [peptide] = 3 mM. Green number near a line indicates its temperature coefficient ($-\Delta\delta/\Delta T$ in ppb/deg).

tion pattern indicates that the N-terminal sequence involves amide NH groups free from intramolecular hydrogen bonding. Thus, the upfield Aib NH should be assigned to the Aib(3)'s. The other NH groups observed were less dependent on temperature, thus being shielded as a result of intramolecular hydrogen bonding (Figure 2). Although the Δ^ZPhe(2) NH was not clearly found, peptides **1**-*m* were shown to adopt a 3_{10}-helical conformation. The influence of $(CD_3)_2SO$ on NH chemical shifts[8f,g,i,10a−d,14e,j,o,p,32] was also investigated in **1**-*2* (Figure S6, Supporting Information). Among the NH resonances, the Aib(3) NH undergoes remarkable shift to a low magnetic field. In contrast, the six NHs of Δ^ZPhe(4)−Aib(9) are essentially maintained by the hydrogen-bond acceptor, also supporting the occurrence of a 3_{10}-helix. Similar temperature dependence of NH chemical shifts in a 3_{10}-helix was seen in peptide **2** (Figure 2).

Computational Simulation of Helical Structures. The helical propensity of **1**-*m* was also investigated from a theoretical point of view. Since Δ^ZPhe- and Aib-containing peptides often take not only a 3_{10}-helix but an α-helix,[14] both helices were considered as initial conformers. Here two orientations of the biphenyl moiety were used, i.e., positive or negative torsion angles (χ^6) about the phenyl−phenylene linkage. Energy minimization was carried out with Gaussian 03[33] by the semiempirical molecular orbital (MO) method (AM1),[33,34] followed by a single-point density functional theory (DFT) [B3LYP/6-31G(d,p)] computation to improve energy precision.[33,35,36]

The structures and energies are summarized in Figure 3[37] and Table 2. In all cases, energy minimization from a 3_{10}-helix maintained 3_{10}-helical structures. Their structural data (torsion angles and hydrogen bond parameters) are summarized in Table S1, Supporting Information. The three peptides of **1**-*m* have almost the same average values of (ϕ, ψ). In each peptide, 3_{10}-helical hydrogen bonds are formed for every *i*th CO and (i + 3)th NH pair. Here average hydrogen-bonding parameters of **1**-*m* are also similar to each other. Thus the structural features of the 3_{10}-helix are not affected by chain length in the current sequences but originate from conformational properties of the Aib and ΔAA residues.

Energy minimization from an α-helix yielded essentially α-helices, but a 3_{10}-helical hydrogen-bonding manner was found

(32) Pitner, T. P.; Urry, D. W. *J. Am. Chem. Soc.* **1972**, *94*, 1399–1400.

(33) (a) *Gaussian 03, Revision C.02* Frisch, M. J. et al. Gaussian, Inc.: Wallingford CT, 2004. (b) For the manual and full references for Gaussian 03, see also: The Official Gaussian 03 Website (http://www.gaussian.com/).

(34) For the AM1 method, see: Dewar, M. J. S.; Zoebisch, E. G.; Healy, E. F.; Stewart, J. J. P. *J. Am. Chem. Soc.* **1985**, *107*, 3902–3909.

(35) For the B3LYP method, see: (a) Becke, A. D. *J. Chem. Phys.* **1993**, *98*, 5648–5652. (b) Stephens, P. J.; Devlin, F. J.; Chabalowski, C. F.; Frisch, M. J. *J. Phys. Chem.* **1994**, *98*, 11623–11627. (c) Lee, C.; Yang, W.; Parr, R. G. *Phys. Rev. B.* **1988**, *37*, 785–789.

(36) Foresman, J. B.; Frisch, Æ. *Exploring Chemistry with Electronic Structure Methods*, 2nd ed.; Gaussian, Inc.: Pittsburgh, PA, 1996; Chapters 6−7.

(37) For molecular graphics in the present paper, see: Thompson, M. A. *ArgusLab 4.0.1*; Planaria Software LLC: Seattle, WA (http://www.arguslab.com).

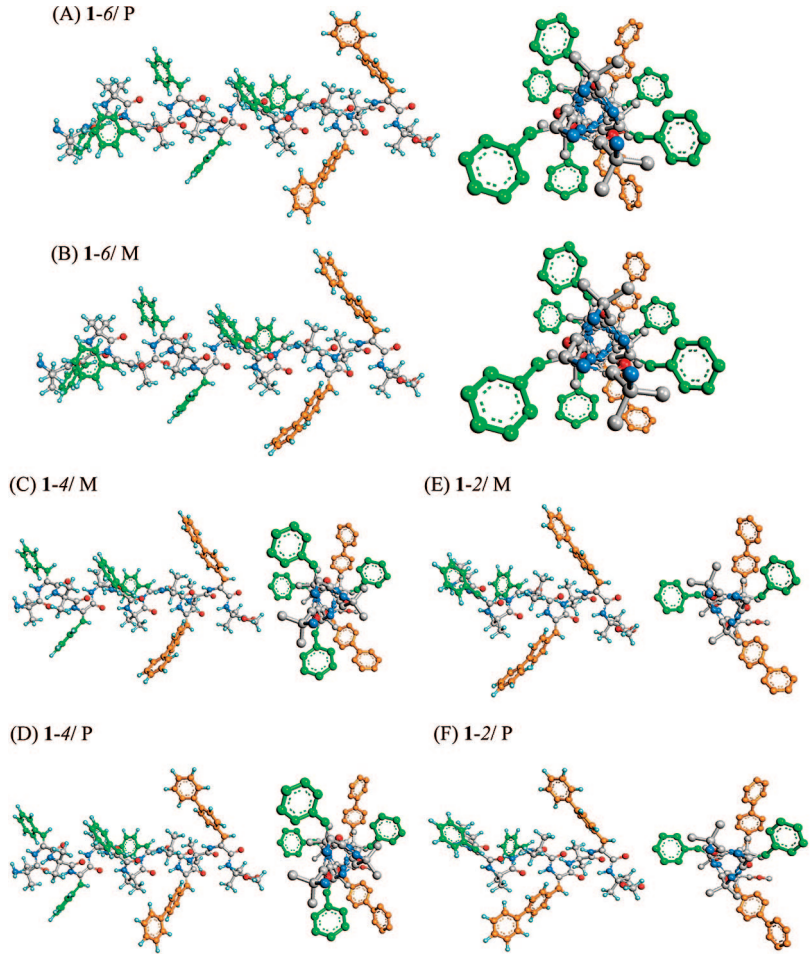

FIGURE 3. Right-handed helical structures of **1**-*m* energy-minimized from a 3_{10}-helix: (A, B) **1**-*6*, (C, D) **1**-*4*, and (E, F) **1**-*2*. M and P stand for the two orientations (χ^6) of the biphenyl groups.

TABLE 2. Energy and Dipole Moment of Peptides 1-*m* Energy-Minimized from a 3_{10}-Helix or an α-Helix[a]

peptide	type of initial helix[b]	biphenyl orientation[c]	energy difference (kcal mol^{-1}) per molecule	energy difference (kcal mol^{-1}) per residues	dipole moment (debye)
1-*6*	3_{10}-helix	P	0.00	0.00	64.7
	3_{10}-helix	M	0.04	0.00	64.7
	α-helix	M	13.66	0.80	67.9
	α-helix	P	15.20	0.89	67.8
1-*4*	3_{10}-helix	M	0.00	0.00	47.3
	3_{10}-helix	P	0.05	0.00	47.3
	α-helix	M	11.29	0.87	48.5
	α-helix	P	12.93	0.99	48.4
1-*2*	3_{10}-helix	M	0.00	0.00	30.2
	3_{10}-helix	P	0.22	0.02	30.2
	α-helix	M	8.66	0.96	30.0
	α-helix	P	10.74	1.19	29.8

[a] These structures are provided in Figure 3 (3_{10}-helix) and Figure S7, Supporting Information (α-helix). The energy minimization was carried out by the AM1 method.[34] Each structure obtained was subjected to single-point DFT computation to yield its energy and dipole moment. [b] For the initial conformation. [c] Negative (M) and positive (P) χ^6 values of the two biphenyl groups in the initial conformation (for the detail, see the experimental section).

in the N-terminal sequence (Figure S7, Supporting Information). As shown in Table 2, the energy difference per residue between structures energy-minimized from a 3_{10}-helix and an α-helix seems to become somewhat smaller with increasing chain length. This prediction might be related to the view that the 3_{10}-/α-helical propensities are often switched by chain length.[38] However, in all cases, the 3_{10}-helices are more stable by 0.8−1.2 kcal mol^{-1} per residues than the α-helices. Such a strong preference for 3_{10}-helix should be attributed to the conformational nature of Aib and ΔAA residues.[14] The biphenyl orientation of M or P seems not to influence the stability of helical structures substantially.

UV Absorption Patterns. Δ^ZPhe-based peptide **3** in chloroform showed a strong absorption band at around 280 nm.[10a] In the Δ^ZBip-based peptide **2** in chloroform, a marked absorption band was observed at longer wavelengths (ca. 310 nm) (Figure S8, Supporting Information). Absorption bands of peptides **1**-*m* should occur through combination of both chromophoric residues. In fact, the absorption maxima of **1**-*m* was between 280 and 310 nm in chloroform (Figure 4), indicating partial overlap of the two absorption bands. A peak shoulder or tail above 320 nm in **1**-*m* is not derived from the Δ^ZPhe residues, as judged from absorption spectrum of **3** (Figure S8, Supporting Information). In other words, CD signals above 320 nm are essentially defined as chiral information of the Δ^ZBip-based segment.

(38) (a) Pavone, V.; Benedetti, E.; Di Blasio, B.; Pedone, C.; Santini, A.; Bavoso, A.; Toniolo, C.; Crisma, M.; Sartore, L. *J. Biomol. Struct. Dyn.* **1990**, *7*, 1321–1331. (b) Karle, I. L.; Flippen-Anderson, J. L.; Gurunath, R.; Balaram, P. *Protein Sci.* **1994**, *3*, 1547–1555. (c) Fiori, W. R.; Miick, S. M.; Millhauser, G. L. *Biochemistry* **1993**, *32*, 11957–11962. (d) Basu, G.; Kuki, A. *Biopolymers* **1992**, *32*, 61–71.

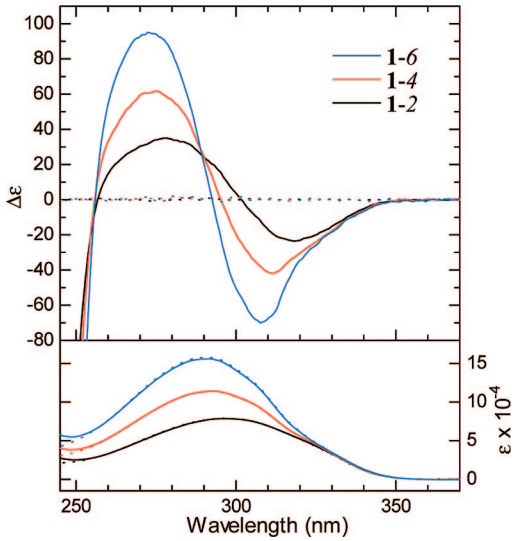

FIGURE 4. Induced CD spectra of peptides **1**-*m* with Boc-L-proline in chloroform: [Boc-L-proline] = 65 mM. The dotted lines indicate those without chiral additive: [**1**-*6*] = 6.3×10^{-2} mM; [**1**-*4*] = 9.0×10^{-2} mM; [**1**-*2*] = 0.13 mM. The bottom panel stands for the corresponding absorption spectra.

Induction of Helix Sense through Noncovalent Chiral Interaction. The achiral sequence **1**-*m* originally shows no CD signals in the absence of chiral stimuli. In contrast, CD signals of **1**-*m* were induced at around 270−320 nm by chiral Boc-amino acid. Figure 4 displays CD spectra of **1**-*m* with Boc-proline in chloroform. In each peptide, a mirror CD pattern was observed between the added enantiomers (Figure S9, Supporting Information). It is obvious that the CD signals are generated from external chiral stimulus. All of the CD spectra, which are essentially identified as exciton splitting patterns, possess clear signals at over 320 nm. Thus chiral induction occurs at both the Δ^ZPhe- and Δ^ZBip-based regions.

N-Terminally protected peptides **1**-*m*, Boc-(Aib-Δ^ZPhe)$_m$-(Aib-Δ^ZBip)$_2$-Aib-OMe (m = 2, 4, and 6), yielded no marked CD signals in the presence of a large excess of Boc-L-proline (Figure S10, Supporting Information). On the other hand, the induced CD intensity of **1**-*m* increased with increasing concentration of Boc-L-proline (Figure S11, Supporting Information). From the plots of $\Delta\varepsilon$ against the additive concentration, the apparent binding constants (K_{app}) for **1**-*m* were estimated to be substantially similar to each other.[39] These additional facts support that the chiral molecule binds the N-terminal sequence to induce the preference for a one-handed helix.

We have proposed the mechanism of NCDE in H-β-Ala- and H-Gly-capped 3_{10}-helical peptides.[10b,c] Hydrogen-bond-free amide NH and amino groups appear inherently in the N-terminal helical motif to participate in the three-point coordination to chiral Boc-amino acid.[10b,c,40] Terminal asymmetric information originating in the complex structure spreads over the helical backbone. A similar mechanism for the chiral induction should be applied to the present case, on the basis of the preceding results. Consequently, the external chiral molecule stimulates the N-terminal sequence to generate a helical sense in the optically inactive backbone. Herein chiral information at the N-terminus reaches the C-terminal Δ^ZBip-based region.

Helical Arrangement of Transition Moments. The TDM of Δ^ZPhe absorption band at around 280 nm was estimated to lie approximately at the phenyl−carbonyl line.[17] In a 3_{10}-helical segment of repeating (X-Δ^ZPhe) units, the nearest TDM pairs are twisted clockwise or counterclockwise. Such a spatial twist enables us to determine the helical sense by the exciton chirality method.[18]

Here, we predicted the TDM for each Δ^ZBip or Δ^ZPhe residue incorporated in peptide **1**-*6* adopting the right-handed 3_{10}-helices. Each ΔAA geometry was extracted from Figure 3 to convert into Ac-Δ^ZBip-NMA or Ac-Δ^ZPhe-NMA. For these N- and C-protected amino acids, the ZINDO/S computation was carried out with Gaussian 03[33,41] to yield their electronic transition parameters of oscillator strength (f) and TDM.

The Δ^ZBip residues showed large f values at around 295−298 nm, while marked f values were seen at around 274−277 nm for the Δ^ZPhe residues. These predicted wavelengths were close to the ones experimentally found in **2** and **3** (Figure S8, Supporting Information), ensuring the validity of the prediction. Each TDM obtained in the velocity form is superimposed on the corresponding right-handed 3_{10}-helix of **1**-*6* (Figure 5). The neighboring TDM pairs are twisted counterclockwise along the right-handed helical axis.[42] Since the energy gap between the Δ^ZBip- and Δ^ZPhe-transition states of each f_{max} is not so large, the exciton chirality method will be valid for the present case.[18] The helical arrangement of TDM will generate split-type CD patterns with a negative peak at longer wavelengths, thus indicating that a right-handed helix is induced by Boc-L-proline. Induction or stabilization of a right-handed helix by Boc-L-amino acid has been demonstrated in N-terminal free helical peptides.[10−12] Therefore both the Δ^ZPhe- and Δ^ZBip-based segments adopt a 3_{10}-helical conformation with the same sense.

Simulation of Theoretical CD Spectra. The preceding analysis reveals that chiral information reaches the Δ^ZBip-based region. Recently, theoretical CD simulation on Δ^ZPhe-containing helical peptides provides deep insights into their conformations.[17d] In the present section, we report similar CD simulation of **1**-*m* and also attempts to discriminate between the 3_{10}-helix and α-helix in Table 2.

Electronic transition-state and chiroptical parameters of **1**-*m* in the right-handed helix were computed by the time-dependent (TD) method of ZINDO/S with Gaussian 03.[33,41−44] The use of these parameters in the velocity form produced the CD spectra as well as absorption profiles (Figure 6).

(39) Nonlinear fitting of the $\Delta\varepsilon$ values at 0−100 mM gave the corresponding K_{app} value: 2.5 × 10 (**1**-*6*), 2.0 × 10 (**1**-*4*), and 1.9 × 10 (**1**-*2*). Similar treatment was done in ref 11c. Likewise, the estimated K_{app} value was 1.7 × 10 (**3**: for 0−102 mM). For these plots, see Figure S11, Supporting Information. While the relationship between $\Delta\varepsilon$ of **3** and the concentration of chiral additive was reported,[10a] the updated data were analyzed. The K_{app} values ranging between 17 and 25 indicate similar interaction for the chiral induction.

(40) For the nature of helix termini in proteins and peptides, see: (a) Aurora, R.; Rose, G. D. *Protein Sci.* **1998**, *7*, 21–38. (b) Baldwin, R. L.; Rose, G. D. *Trends Biochem. Sci.* **1999**, *24*, 26–33. (c) Harper, E. T.; Rose, G. D. *Biochemistry* **1993**, *32*, 7605–7609. (d) Seale, J. W.; Srinivasan, R.; Rose, G. D. *Protein Sci.* **1994**, *3*, 1741–1745. (e) Karpen, M. E.; DeHaseth, P. L.; Neet, K. E. *Protein Sci.* **1992**, *1*, 1333–1342.

(41) For the ZINDO/S method, see: (a) Ridley, J. E.; Zerner, M. C. *Theor. Chim. Acta* **1973**, *32*, 111–134. (b) Ridley, J. E.; Zerner, M. C. *Theor. Chim. Acta* **1976**, *42*, 223–236. (c) Zerner, M. C.; Loew, G. H.; Kirchner, R. F.; Mueller-Westerhoff, U. T. *J. Am. Chem. Soc.* **1980**, *102*, 589–599. (d) Thompson, M. A.; Zerner, M. C. *J. Am. Chem. Soc.* **1991**, *113*, 8210–8215.

(42) A similar helical arrangement of each TDM in the length form was obtained; see Figure S12, Supporting Information.

(43) For the ZINDO-based CD simulation, see: (a) Telfer, S. G.; Tajima, N.; Kuroda, R. *J. Am. Chem. Soc.* **2004**, *126*, 1408–1418. (b) Ankai, E.; Sakakibara, K.; Uchida, S.; Uchida, Y.; Yokoyama, Y.; Yokoyama, Y. *Bull. Chem. Soc. Jpn.* **2001**, *75*, 1101–1108. (c) Kawai, M.; Nagai, U.; Inai, Y.; Yamamura, H.; Akasaka, R.; Takagi, S.; Miwa, Y.; Taga, T. *Biopolymers* **2005**, *80*, 186–198. (d) Fujii, T.; Shiotsuki, M.; Inai, Y.; Sanda, F.; Masuda, T. *Macromolecules* **2007**, *40*, 7079–7088.

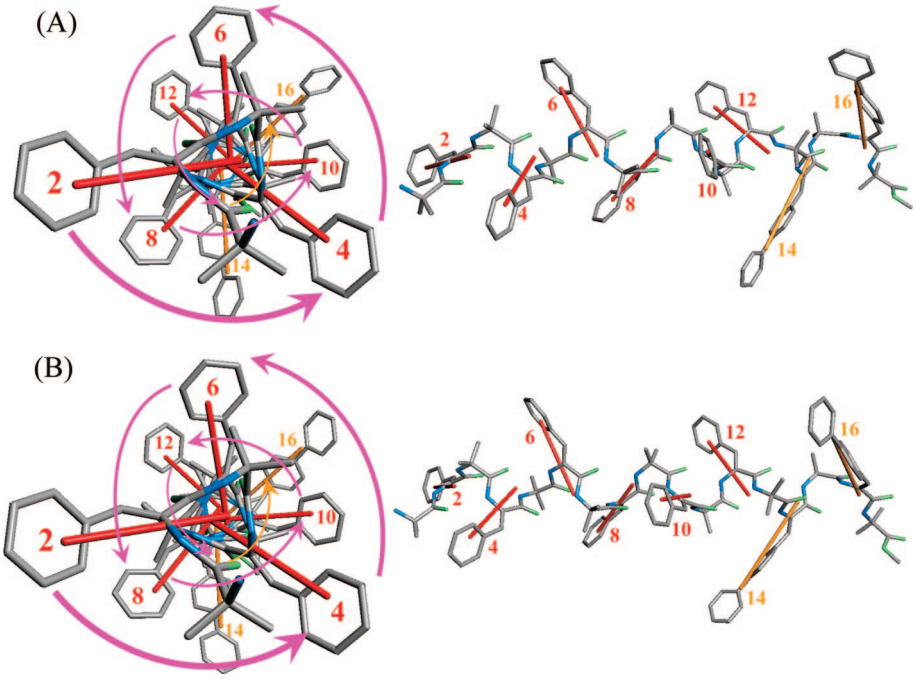

FIGURE 5. Spatial arrangement of each ΔAA residue TDM (in the velocity form) along the right-handed 3_{10}-helix of **1**-*6*: (A) and (B) correspond to Figure 3A and 3B with P- and M-orientations of the Δ^{Z}Bip side chains. The right-handed helix produces a left-handed twist of the neighboring moments with respect to the helical axis.

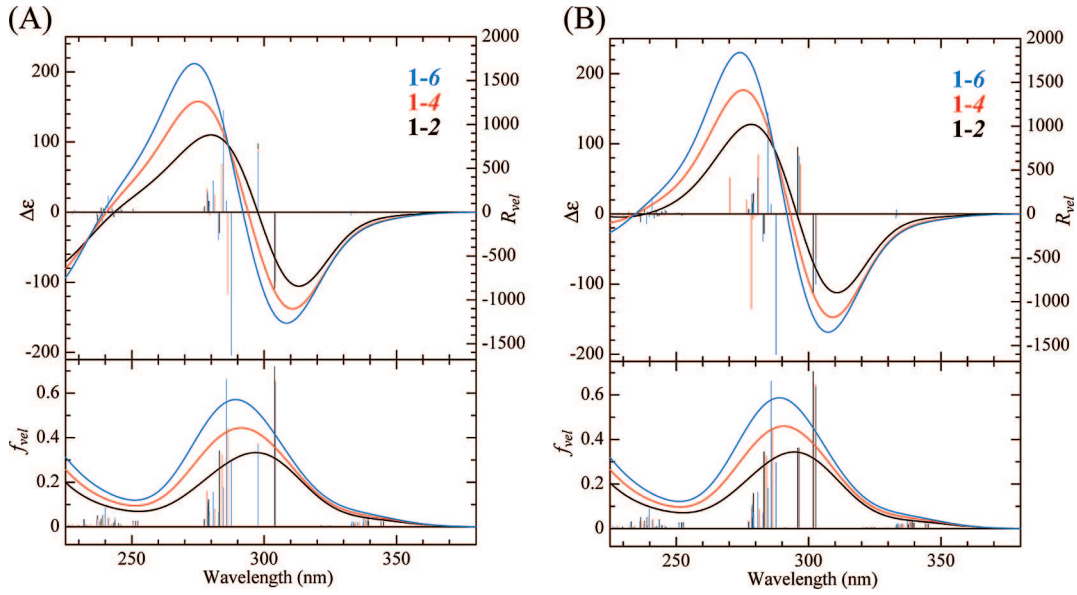

FIGURE 6. Electronic transition parameters and simulated CD spectra of **1**-*m* in the 3_{10}-helices (Figure 3) with (A) M- and (B) P-orientations of the two Δ^{Z}Bip side chains.

When peptides **1**-*m* assume the right-handed 3_{10}-helical structures, the simulated spectra (Figure 6) resemble the experimental ones (Figure 4) in the following points: (i) Peptides **1**-*m* produced essentially split-type CD patterns with negative signals at longer wavelengths. (ii) The CD amplitude per molecule monotonically increased with the chain length. (iii) Both maximal and minimal positions of the split CD patterns were shifted to shorter wavelengths by the increasing chain length. The corresponding absorption profiles underwent a similar blue shift. These spectral changes are readily understood in terms of increasing contribution of the Δ^{Z}Phe-based transition states. (iv) There appeared to be an isodichroic point at a positive $\Delta\varepsilon$ value of a second Cotton effect.

The biphenyl orientation of M or P seems not to influence CD patterns at over 250 nm essentially. Similarities between the experimental and theoretical CD spectra in the 3_{10}-helices (Figure 6) disappear in the α-helices (Figure 7). That is, the α-helices of **1**-*m* mostly produced not a simple split pattern but

(44) The TD SCF MO method for simulation of CD spectra has been recently advanced: (a) Stephens, P. J.; McCann, D. M.; Devlin, F. J.; Cheeseman, J. R.; Frisch, M. J. *J. Am. Chem. Soc.* **2004**, *126*, 7514–7521. (b) Furche, F.; Ahlrichs, R.; Wachsmann, C.; Weber, E.; Sobanski, A.; Vögtle, F.; Grimme, S. *J. Am. Chem. Soc.* **2000**, *122*, 1717–1724. (c) Autschbach, J.; Ziegler, T.; Gisbergen, S. J. A.; Baerends, E. J. *J. Chem. Phys.* **2002**, *116*, 6930–6940. (d) Diedrich, C.; Grimme, S. *J. Phys. Chem. A* **2003**, *107*, 2524–2539. (e) Brown, A.; Kemp, C. M.; Mason, S. F. *J. Chem. Soc.* **1971**, 751–755.

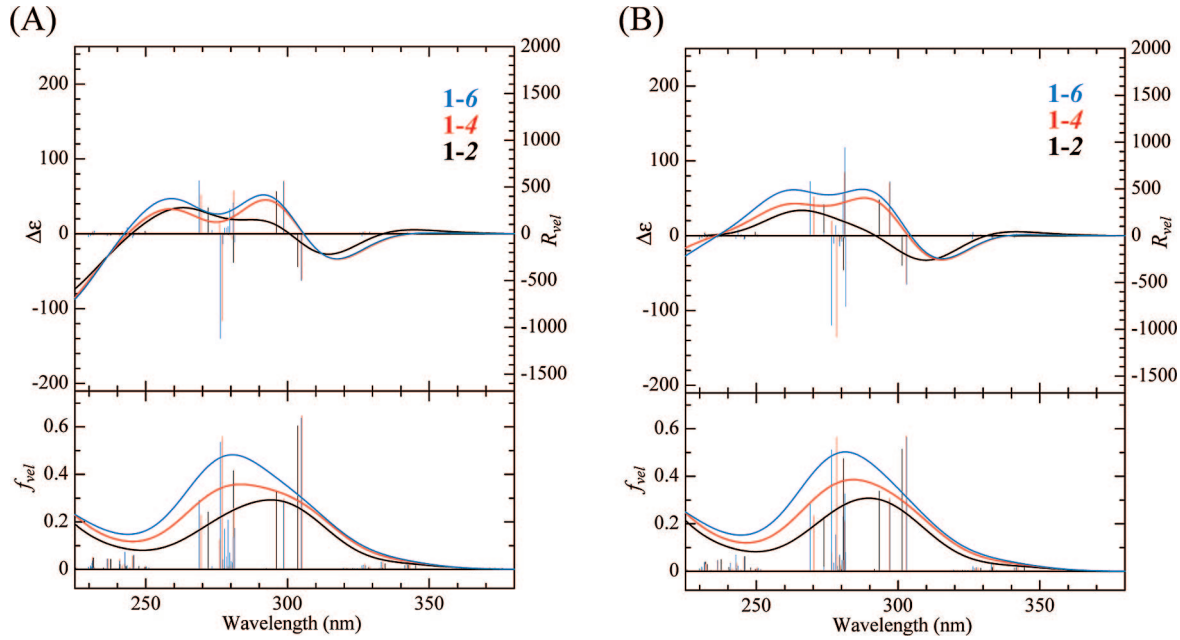

FIGURE 7. Electronic transition parameters and simulated CD spectra of **1**-*m* in the α-helices (Figure S7, Supporting Information) with (A) M- and (B) P-orientations in the two Δ^ZBip side chains.

a more complex one with positive-positive-negative signals for shorter to longer wavelengths (Figure 7). In addition, the CD intensities of the α-helices were considerably smaller than those of the 3_{10}-helical cases. A marked difference between the CD intensities of the 3_{10}-helix and α-helix indicates that the transformation from 3_{10}-helix to α-helix does not occur in the three peptides. They all adopt a 3_{10}-helical structure in solution as displayed in Figure 3. We have also checked the validity of the current CD simulation.[45]

Similarly, CD spectra were simulated for peptides **2** and **3** that take 3_{10}-helical or α-helical conformations (Figures S14−S17, Supporting Information). The absorption profile of **2** was shifted to a longer wavelength by ca. 20 nm compared with that of **3**, supporting the experimental trend of the absorption spectra (Figure S8, Supporting Information). The right-handed 3_{10}-helix of **2** and **3** showed a split CD pattern with negative signals at longer wavelengths. The pattern agrees with that induced by Boc-L-proline, which thus leads to a right-handed helix of **2** as commonly observed in **1**-*m*, **3**, and other analogous peptides.[10,12]

Peptide **1**-*6* forms a 3_{10}-helical backbone characterized by about five turns and a total length of ca. 33 Å [Aib(1) N−Aib(17) N]. An increase in peptide chain length often switches a 3_{10}-helix to an α-helix.[38] In fact, a 3_{10}-helix is usually present as a short segment in proteins.[23,40e] Oligopeptides based on α,α-disubstituted residues or *β*-substituted α,*β*-didehydroresidues also form a 3_{10}-helical structure (in some cases, α-helix).[14] Whereas a long 3_{10}-helical chain is found in sequences of 10 residues or more,[46] little is known about the case of 16 residues or more.[47] Thus we have proposed that the 17-mer sequence composed of Aib and ΔAA residues favors a 3_{10}-helix in solution.

Energies and CD Spectra for Helix Inversion. The preceding CD simulation supports that chiral information received at the N-terminus reaches the 16th position. However, achiral residues such as Aib and Δ^ZPhe can take equally both screw senses to reverse helical sense. It has been demonstrated that such helix inversion occurs at an achiral residue along a peptide sequence.[2a−e,13a] For instance, a right-handed α-helical motif in proteins is often accompanied with its C-terminal Gly residue taking a left-handed conformation.[2a−e,j,k] Recently, we discovered that chiral/achiral block sequence undergoes helix inversion at around the boundary to generate a heterochiral helix.[13a]

Correspondingly, the helix sense of **1**-*6* might be switched at the Δ^ZBip-based region. To clarify the point, several heterochiral helices were generated as follows. In the initial conformers, the position for starting helix inversion (PHI) was set to the 13th, 15th, or 16th residue from the N-terminus. Energy minimization from each conformer yielded the corresponding heterochiral structure (Figure S18, Supporting Information). Their energies and dipole moments obtained through single-point DFT computation are provided in Table 3. It also contains the most stable 3_{10}-helix shown in Table 2 (the helix inversion at the C-terminal Aib is defined as PHI = 17th). The heterochiral helices of PHI = 13th, 15th, and 16th were less

(45) CD simulation at the semiempirical MO level (ZINDO/S) has been verified through comparison with CD simulation at a higher level. Here TD DFT was applied to three smaller fragments of **1**-*2*: Ac-Δ^ZPhe-Gly-Δ^ZPhe-NMA, Ac-Δ^ZPhe-Gly-Δ^ZBip-NMA, and Ac-Δ^ZBip-Gly-Δ^ZBip-NMA (Ac = acetyl; NMA = *N*-methylamide) were produced by using the atomic coordinates extracted from the 3_{10}-helical structures of **1**-*2* (Figure S13, Supporting Information). CD spectra of these short helical fragments, obtained from both the DFT and ZINDO/S methods, yielded split-type CD patterns essentially (Figure S13, Supporting Information). Split CD patterns were shifted to a longer wavelength with increasing the aromatic size of ΔAA residue. At the DFT method, there is no essential difference between the velocity- and length-based CD spectra of which all are identified as split-type patterns. Meanwhile, at the ZINDO/S method, the velocity-based CD spectra are regarded as split types, but such split patterns are distorted in the length-based spectra of **1**-*4* and **1**-*2*. As a result, CD profiles at the DFT level were essentially obtained by using velocity-based parameters at the ZINDO/S level. This supports the validity of the current CD simulation of **1**-*m*.

(46) For instance, see: (a) Toniolo, C.; Crisma, M.; Bonora, G. M.; Benedetti, E.; Di Blasio, B.; Pavone, V.; Pedone, C.; Santini, A. *Biopolymers* **1991**, *31*, 129–138. (b) Gessmann, R.; Brückner, H.; Petratos, K. *J. Pept. Sci.* **2003**, *9*, 753–762. (c) Rudresh; Gupta, M.; Ramakumar, S.; Chauhan, V. S. *Biopolymers* **2005**, *80*, 617–627. (d) Ramagopal, U. A.; Ramakumar, S.; Mathur, P.; Joshi, R.; Chauhan, V. S. *Protein Eng.* **2002**, *15*, 331–335. (e) Pavone, V.; Di Blasio, B.; Santini, A.; Benedetti, E.; Pedone, C.; Toniolo, C.; Crisma, M. *J. Mol. Biol.* **1990**, *214*, 633–635.

(47) For instance, see: Malcolm, B. R.; Walkinshaw, M. D. *Biopolymers* **1986**, *25*, 607–625.

TABLE 3. Energy and Dipole Moment of 1-*6* Energy-Minimized from Several Helix Inversions[a]

peptide	position for starting helix inversion (PHI)[b]	biphenyl orientation[c]	energy difference (kcal mol^{-1})[d] per molecule	energy difference (kcal mol^{-1})[d] per residues	dipole moment (debye)
1-*6*	17th[d]	P	0.00	0.00	64.7
	13th	M	5.28	0.31	63.6
	15th	M	5.92	0.35	63.0
	13th	P	6.10	0.36	63.3
	15th	P	6.53	0.38	63.0
	16th	M	9.67	0.57	62.6
	16th	P	9.98	0.59	62.7

[a] Energy minimization from 3_{10}-helices containing a helical reversal point was carried out by the AM1 method.[33,34] Each structure obtained was subjected to single-point DFT computation to yield its energy and dipole moment.[33,35] [b] PHI at initial conformations. [c] Phenyl−phenylene twist in the two biphenyl groups. [d] From the lowest energy in Table 2.

stable than the 3_{10}-helix of PHI = 17th but energetically more favorable than the α-helices in Table 2. The preference for PHI = 17th might be relevant to the fact that the C-terminal residue of Aib-OMe often tends to switch the screw sense.[14d,h,15b]

CD spectra simulated for these heterochiral helices are displayed in Figure S19, Supporting Information. They showed positive or small negative signals at 310−330 nm. Positive CD peaks of PHI = 13th, 15th, and 16th appeared at shorter wavelengths (260−280 nm) with smaller intensities compared with the case of PHI = 17th. The decrease in CD intensity will be responsible for the opposite chiral information between the Δ^ZPhe- and Δ^ZBip-based sequences. CD spectra of **1**-*6* should discriminate between PHI = 13th−16th and PHI = 17th. The analysis of the theoretical CD spectra confirms that the same helix sense reaches the 16th residue in **1**-*6*.

Conclusions

The end-to-end transfer of chiral information along a peptide chain not only gains deep insight into propagation of a one-handed helicity in proteins but also provides a primitive model for allosteric process in biological structure and function.[21] Concerning the latter issue, a remote control along a single chain has been elegantly studied, but a long-range allosteric effect is rarely found in a synthetic unimolecule.[19] For a unique example, the asymmetric reaction for one terminal moiety of an achiral segment is controlled by chiral moiety covalently bound to the opposite terminus.[19a] Here, both the termini are separated by a distance of over 25 Å.[19a] As another example, when a chiral residue is covalently incorporated into one terminus of an achiral peptide, CD signals are induced in a chromophoric group at the opposite end.[8f] In addition, chiral information transfers along duplex chains of peptide nucleic acids.[8a] In contrast, little is known about the precise tracing of *noncovalent* chiral information in a synthetic unimolecule.[19b]

Here we have synthesized Δ^ZPhe-based peptides anchoring a pair of the Δ^ZBip residues to the C-terminal region. CD spectroscopy combined with exciton chirality method[18] and theoretical simulation[17d] has effectively traced the route. That is, a right-handed helix is induced in the optically inactive peptides of 9-mer to 17-mer by a Boc-L-proline stimulus to their N-terminal sequence. The dynamic chiral information reaches substantially their C-terminal region [16th position in the 17-mer (**1**-*6*)]. This provides clear evidence for the NCDE, in which an external molecule binding to the N-terminal region can control the chiroptical signals and helical sense of the C-terminal region.

In the 17-mer (**1**-*6*), the first to 16th residues are separated by a distance of more than 30 Å, which is regarded as a long-range allosteric effect in a synthetic unimolecule.[19a] Our model might propose a basic element for artificial molecular motors or machines based on helical gears.[22a,48] External chiral manipulation of the terminal gear can control the direction and power of the internal rotation of the opposite remote gear.

The noncovalent chiral information can govern the helical sense of the optically inactive peptides, even if they have a considerably long chain. From the thermodynamic viewpoint, peptide **1**-*6* adopts right-handed and left-handed 3_{10}-helices in equilibrium of solution. In our previous works,[10−12] CD intensity induced in N-terminal-free peptides based on -(Δ^ZPhe-X)$_4$- depends on their N-terminal residue, chiral additive, its concentration, and environmental factors (solvent or temperature).[10−12] Our present findings confirm that change in the induced CD intensity is responsible for a varying ratio of the two helical contents, because each helix does not reverse up to the 16th residue.

Experimental Section

Synthesis. Synthetic route and characterization of peptides **1**-*m* and **2** are provided in Supporting Information.

Spectroscopy. Spectroscopic measurements were performed basically according to refs 11d and 13a. CD data were acquired at ambient temperature on a CD spectrometer. Data smoothing was done for noise-reduced CD spectra. UV absorption spectra were obtained on the CD spectrometer or a UV−vis spectrometer.

Sample solution was prepared as follows.[11c] Concentration of **1**-*m*, **2**, and **3** was determined by using their maximal molar extinction coefficients (ε_{max}) at 270−310 nm of analogous and model compounds: ε_{max} of **1**-*6* = 15.8 × 10^4 (from Boc-protected **1**-*6* at 292 nm); ε_{max} of **1**-*4* = 11.4 × 10^4 (from Boc-protected **1**-*4* at 293.5 nm); ε_{max} of **1**-*2* = 7.9 × 10^4 (from Boc-protected **1**-*2* at 297 nm); ε_{max} of **2** = 2.6 × 10^4 per Δ^ZBip (from Boc-Aib-Δ^ZBip-Aib-OMe at 296 nm); ε_{max} of **3** = 1.8 × 10^4 per Δ^ZPhe (from analogous peptides[10b,17d]).

A chloroform solution of an N-terminal free peptide was prepared at a given concentration. Then a prescribed volume of the solution was added to an amount of chiral molecule to give its desirable concentration. Here, the added volume was assumed not to change throughout the mixing or further handling processes. Basically, the $\Delta\varepsilon$ value was calibrated with (1*R*)-10-camphorsulfonic acid ammonium salt (CSAAS) purchased from Aldrich (Milwaukee, WI). [On the other hand, the calibration factor of $\Delta\varepsilon$ was somewhat smaller when commercially available (1*S*)-CSAAS (Sigma Aldrich Japan; Tokyo, Japan) was used for CD calibration.[49] If using the latter standard, the $\Delta\varepsilon$ value should be multiplied by a factor of ca. 0.93.] In addition, the sample solutions of **1**-*2*, **1**-*4*, and **1**-*6* were prepared with the same solvent to minimize CD spectral changes caused from different conditions.

Basically according to ref 13a, ^{1}H NMR spectra were obtained on 600- or 200-MHz ^{1}H NMR spectrometers. 2D-NOESY spectra were acquired on the 600-MHz NMR spectrometer by using the pulse program ("noesytp"[50]) usually with a mixing time of 0.4 or

(48) (a) Kottas, G. S.; Clarke, L. I.; Horinek, D.; Michl, J. *Chem. Rev.* **2005**, *105*, 1281–1376. (b) Feringa, B. L. *Acc. Chem. Res.* **2001**, *34*, 504–513. (c) Kinbara, K.; Aida, T. *Chem. Rev.* **2005**, *105*, 1377–1400. (d) Kelly, T. R. *Acc. Chem. Res.* **2001**, *34*, 514–522.

(49) Absolute CD values of (1*S*)- and (1*R*)-CSAAS were assumed to be the same. For the calibration with (1*S*)-CSAAS, see the spectroscopic manual of JASCO J-820. See also: Takakuwa, T.; Konno, T.; Meguro, H. *Anal. Sci.* **1985**, *1*, 215–218.

(50) Bodenhausen, G.; Kogler, H.; Ernst, R. R. *J. Magn. Reson.* **1984**, *58*, 370–388.

(51) Wüthrich, K. *NMR of Proteins and Nucleic Acids*; John Wiley and Sons: New York, 1986.

0.2 s. (For NMR guidance of biopolymers, see ref 51.) NMR processing and analysis were done with the Bruker software [Bruker BioSpin, Karlsruhe, Germany; Tsukuba, Japan] or SPINWORKS.[52] FT-IR absorption and MALDI-TOF mass spectra were obtained essentially according to ref 13a.

Conformational Energy Calculation. The helical structure of **1**-*m* (m = 2, 4, and 6) was predicted by energy calculation. The initial backbone (ϕ, ψ, ω) of the 2nd−16th residues was set to a right-handed 3_{10}-helix (−60°, −30°, 180°)[53] or α-helix (−57°, −47°, 180°).[54] (Although the right-handed helix was commonly chosen here, it must be energetically identical to the enantiomeric left-handed helix due to the achiral sequence.) The C-terminal Aib-OMe adopted the corresponding left-handed helix, because such a helical reversal at the C-terminus is widely found in natural or synthetic sequences.[2a,b,14d,f,h,15b]

According to the theoretical CD analysis,[17d] the Δ^ZPhe phenyl planes along a 3_{10}-helical backbone of (Aib-Δ^ZPhe)$_n$ prefer an orientation roughly parallel to the helical axis. Thus the χ^2 angle of the Δ^ZPhe and Δ^ZBip residues was set to −40° for a right-handed helix.[55] The two Δ^ZBip residues took the same side-chain orientation of $\chi^6 = -45°$ (M) or +45° (P).[56] Energy minimization of these initial conformations[57] was carried out with Gaussian 03 at the AM1 method,[33,34] in which all structural parameters varied. For each optimized structure, single-point computation at the B3LYP/6-31(d,p) level was performed to improve the energy accuracy.[33,35,36]

Heterochiral helical structures of **1**-*6* were also simulated. The initial conformation of PHI = *i*th took a right-handed 3_{10}-helix (−60°, −30°, 180°) for the second to (i − 1)th residues, and a left-handed 3_{10}-helix (+60°, +30°, 180°)[53] for the *i*th to 17th residues. In each initial conformer, the χ^2 of Δ^ZBip residues in the left-handed helical segment was set to 40°, while the other Δ^ZPhe and Δ^ZBip residues retained the original χ^2 value (−40°). The χ^6 of the two Δ^ZBip residues was also set to −45° (M) or +45° (P).[56] As mentioned above, each heterochiral helix was energy-minimized at the AM1 level to re-evaluate its energy at the single-point DFT with Gaussian 03.[33−36]

Computation of Theoretical CD Spectra. CD spectra of helical conformations were simulated basically according to ref 17d and 43d. A combination of semiempirical MO (ZINDO/S) and TD methods, by using the keyword of "zindo" and "td" in Gaussian 03, gave electronic-transition and chiroptical parameters such as the rotary strength (R) and f.[17d,33,41,43d] Under limited computational time and memory, higher occupied and lower unoccupied MOs were considered for the configuration interaction (CI). The CI number was calculated from 0.27 × the total atomic orbital (AO) number used for the ZINDO/S computation. That is, the total AO number of **1**-*6* (755) yielded 204 (higher occupied) × 204 (lower unoccupied) for the CI number and similarly, 160 × 160 for **1**-*4* (591) and 116 × 116 for **1**-*2* (427). In each case, the low-energy transition states of 160 were predicted together with the respective R and f.

Gaussian 03 offers R and f values in the length-based and velocity-based forms.[33] We employed the velocity-based parameters of R and f due to the origin-independent nature.[44] In fact, the velocity-based CD spectra of 3_{10}-helical peptides **1**-*m* (Figure 6) yielded split patterns that well reproduced their experimental ones, whereas the split patterns were distorted in the length-based spectra.

Simulated CD spectra were drawn with a Gaussian-type function based on wavelength scale by using each R value and its transition position.[17d,18b,43,44] A similar Gaussian function based on wavelength scale was used with the velocity-based f to estimate the corresponding absorption profile, of which the vertical scale was expressed in arbitrary unit.[18b,43d] In all cases, a half Gaussian (1/e)-bandwidth (Δ/2) was assumed to be 20 nm, being larger than 14 nm in our previous work.[17d] The use of such a large (Δ/2), as a result, yielded absorption profiles that visually reflected experimental ones.

Furthermore, CD simulation at TD DFT [B3LYP/6-31(d,p)] level was carried out for small fragments of **1**-*2* on Gaussian 03 as mentioned in ref 45. Here R and f parameters of 40 low-energy states were estimated to reproduce CD spectra in a manner similar to the above method.

Acknowledgment. This work was partially supported by the projects (nos. 19550163 and 16550142) of the Ministry of Education, Culture, Sports, Science, and Technology of Japan (MEXT).

Supporting Information Available: FT-IR absorption spectra of **2** and **3**; ^{1}H NMR and 2D NOESY spectra of **1**-*m*; solvent-composition dependence of NH chemical shifts of **1**-*2*; average values of selected torsion angles and hydrogen-bonding parameters of **1**-*m* in 3_{10}-helix; right-handed helical structures of **1**-*m* energy-minimized from an α-helix; CD spectra of **2** or **3** with and without Boc-L-proline; induced CD spectra of **1**-*m* with Boc-D-proline or Boc-L-proline; CD spectra of Boc-protected **1**-*m* with Boc-L-proline; relationship between the CD intensity ($\Delta\varepsilon$) of **1**-*m* and **2** and the concentration of Boc-L-proline; spatial arrangements of each ΔAA residue TDM (in the length form) along the right-handed 3_{10}-helix; electronic transition state parameters and simulated CD spectra of Ac-Δ^ZPhe-Gly-Δ^ZPhe-NMA, Ac-Δ^ZPhe-Gly-Δ^ZBip-NMA, and Ac-Δ^ZBip-Gly-Δ^ZBip-NMA; right-handed helical structures of **2** and **3** energy-minimized from a 3_{10}-helix or from an α-helix; electronic transition state parameters and simulated CD spectra of **2** and **3** in the 3_{10}-helix and α-helix; heterochiral helical structures of **1**-*6* energy-minimized with PHI = 13th, 15th, and 16th; electronic transition state parameters and simulated CD spectra of **1**-*6* in the heterochiral helices; MALDI-TOF mass spectra of **1**-*m* and **2**; synthetic route and characterization of **2**; synthetic route and characterization of **1**-*m*; additional references and notes. This material is available free of charge via the Internet at http://pubs.acs.org.

JO801686M

(52) Marat, K. *SpinWorks*; University of Manitoba: Canada, 1999−2006 (http://www.umanitoba.ca/chemistry/nmr/spinworks/index.html).

(53) (a) Paterson, Y.; Rumsey, S. M.; Benedetti, E.; Némethy, G.; Scheraga, H. A. *J. Am. Chem. Soc.* **1981**, *103*, 2947–2955. (b) Venkatachalam, C. M. *Biopolymers* **1968**, *6*, 1425–1436.

(54) (a) Arnott, S.; Dover, S. D. *J. Mol. Biol.* **1967**, *30*, 209–212. (b) Arnott, S.; Wonacott, A. J. *J. Mol. Biol.* **1966**, *21*, 371–383. (c) IUPAC-IUB Commission on Biochemical Nomenclature. *Biochemistry* **1970**, *9*, 3471−3479. For the definition of torsion angles for peptide conformation, see ref 54c.

(55) (a) Ajò, D.; Casarin, M.; Granozzi, G. *J. Mol. Struct. (THEOCHEM)***1982**, *86*, 297−300. (b) For the side chain conformation (χ^2) of ΔAA residues, see also ref 25c.

(56) (a) Häfelinger, G.; Regelmann, C. *J. Comput. Chem.* **1987**, *8*, 1057–1065. (b) Tsuzuki, S.; Tanabe, K. *J. Phys. Chem.* **1991**, *95*, 139–144.

(57) For the modeling, see ref 13a. For the replacement of Δ^ZPhe-phenyl group by the biphenyl group, see: *GaussView 3.09*, Dennington, R., III.; Keith, T.; Millam, J.; Eppinnett, K.; Hovell, W. L.; Gilliland, R. Semichem, Inc.: Shawnee Mission, KS, 2003.